ISSN: 2977-0041

Research Article

Journal of Material Sciences and Engineering Technology

Preparation of New Nanofiber Conducting Scaffold-Based Polyaniline and Polypyrrole Grafted on Chitosan with Antibacterial Properties

Sama Sadat Hosseini[1*], Seyed Hossein Hosseini[2*]

[1]*Department of pharmaceutical, Nika Pooyesh Industrial Research Institute, Tehran, Iran*

[2]*Department of Chemistry, Nika Pooyesh Industrial Research Institute, Tehran, Iran*

[*]**Corresponding author**

Sama Sadat Hosseini, Department of pharmaceutical, Nika Pooyesh Industrial Research Institute, Tehran, Iran.

Seyed Hossein Hosseini, Department of Chemistry, Nika Pooyesh Industrial Research Institute, Tehran, Iran.

Received: September 05, 2025; **Accepted:** September 15, 2025; **Published:** September 22, 2025

ABSTRACT

Conducting polymers can play a very important role in drug delivery and antibacterial properties due to their unique structure. In this research, first a new chitosan (Cs)-based copolymer graft on which polyaniline (PANI) and polypyrrole (PPy) were grafted was produced. Then, using phytic acid as a crosslinking agent, a new conducting scaffold was made in the form of nanofibers, Poly (Cs-g-PANI-g-PPy). This scaffold was characterized using FT-IR and UV-Visible. Its surface morphology was studied by FTSEM imaging. Its electrical conductivity and percentage of grafting were measured by the four-point method and the corresponding equations, respectively. This composite biopolymer has many good antibacterial properties. These properties were investigated on Pseudomonas aeruginosa, Klebsiella pneumonia as gram-negative and Staphylococcus aureus as gram-positive as a common bacterium in skin and bone by two methods, disk diffusion and minimum inhibitory concentration (MIC). The scaffold's efficacy was quantified, demonstrating a dose-dependent response. The unique multi-grafted architecture is proposed to enhance antibacterial action through synergistic electrostatic disruption and redox-mediated reactive oxygen species (ROS) generation, offering a potent platform against multidrug-resistant pathogens. Cs-g-PANI-g-PPy nanofiber scaffold in concentrations of about 50 µg had a significant antimicrobial effect against all tested bacteria. The results show the higher antimicrobial activity of polymer against the gram-negative rather than gram-positive bacteria. Obviously, the prepared scaffold will have a very good ability to carry drugs and play a role in the treatment of many diseases.

Keywords: Interfacial Polymerization, Graft Copolymer, Chitosan, Polyaniline, Polypyrrole, Antimicrobial, Scaffold

Introduction

Conducting polymers (CPs) are smart polymers that have a wide variety of applications in various industries, including sensors [1], absorption of electromagnetic waves [2] photocatalysts [3], organic electronic devices [4], solar cells [5], nuclear radiation protection [6]. Recently, they have also found many applications in the medical industry, such as antibacterial, anticancer, artificial muscles, and smart drug delivery [7,8].

On the other hand, polymer scaffolds have made good progress in recent years. These compounds have given new properties to composite polymers and therefore have expanded their applications. Polymer scaffolds based on natural polymers have various applications in medical and pharmaceutical industries [9]. Chitosan (Cs) also has antibacterial properties and is widely used in polymer scaffolds [10]. These polymers are biocompatible and degrade gradually in biological environments, and this makes these compounds suitable for antibacterial gels [11], smart drug delivery [12] and bone repair [13]. The molecular structure of Cs and its scaffolds is weak and has less resistance in food and biological environments. Therefore, these compounds should be strengthened for more resistant properties, such as skin repair due to burns or bone repair. Polyaniline (PANI) and polypyrrole (PPy) are the most widely used CPs, which are easy to synthesize and have high electrical conductivity. In the past research, we prepared polymer gels obtained from Cs and PANI co-polymer grafts, which obtained very good results in terms

Citation: Sama Sadat Hosseini, Seyed Hossein Hosseini. Preparation of New Nanofiber Conducting Scaffold-Based Polyaniline and Polypyrrole Grafted on Chitosan with Antibacterial Properties. J Mat Sci Eng Technol. 2025. 3(3): 1-7. DOI: doi.org/10.61440/JMSET.2025.v3.71

of antibacterial properties and skin repair [8]. A more detailed description of biomedical engineering and its applications can be found in more sources [14].

The selection of chitosan as the foundational biopolymer is strategic, leveraging its inherent biocompatibility, biodegradability, and intrinsic cationic nature that disrupts bacterial membranes. However, its mechanical fragility and limited electrical conductivity restrict its application in advanced electro-active biomedicine [15]. Grafting synthetic conducting polymers like PANI and PPy onto the chitosan backbone presents an elegant solution to this limitation, creating a hybrid material that synergizes the best properties of both components. PANI is renowned for its excellent environmental stability and tunable conductivity, while PPy offers high conductivity and ease of synthesis in aqueous media. Their combination within a single grafted copolymer can lead to beneficial electronic interactions and a more versatile material. The transition from a bulk graft copolymer to a nanofibrous scaffold, as achieved here using phytic acid, represents a critical advancement [16]. Nanofibrous architectures, reminiscent of the native extracellular matrix (ECM), provide a high surface-area-to-volume ratio, significantly enhancing cell adhesion, proliferation, and nutrient exchange—properties paramount for tissue engineering scaffolds. Phytic acid, a naturally derived polyphosphate, serves a dual role: as a crosslinker stabilizing the chitosan matrix and as a dopant for both PANI and PPy, simultaneously enhancing the scaffold's mechanical integrity and electrical conductivity [17]. This research fills a notable gap by systematically developing and characterizing this novel multi-component, electro-active nanofibrous system and rigorously evaluating its antibacterial potency against clinically relevant pathogens, thereby establishing its potential for next-generation smart wound dressings and infected tissue repair implants.

In the previous research, we have prepared different conducting polymers with different nanostructures, each of which has different characteristics and properties [1,7,18,19].

In this research work, for the first time, we are trying to prepare a polymer scaffold based on a copolymer graft of PANI and PPy on chitosan with nanofiber (NF) structure (Cs-g-PANI-PPy-NF). In addition to better physical resistance than other polymer scaffolds based on natural polymers, this polymer has properties such as electrical conductivity, the ability to carry medicine, and skin and bone repairs. The overall reaction scheme is shown in Figure 1. In this scheme, due to the complexity of the chemical formulas, the scaffold building is shown schematically.

Experimental

Materials and Methods

The sample of pure chitosan was obtained from Fluka chemical company. Its degree of deacetylation is >85% and the molecular weight 600,000. Aniline and pyrrole monomers (Merck, Germany) were distilled under reduced pressure and stored blew 5˚C. The dodecylbenzene sulfonic acid (DBSA), ammonium persufate (APS) and phytic acid sodium salt (PA) were purchased from Merck (Germany). Acetic acid (AA) glacial was purchased from Fisher Scientific (Germany). Cell biology reagents were purchased from Sigma-Aldrich. A round-shaped papers with 10 mm diameter was prepared by Padtan Teb, Iran. Other materials purchased from Merck Company and used correctly. Double distilled water used in all experiments. Fourier transform infrared spectroscopy (FTIR) spectrum was recorded by Termo Co. WCOF-510 (USA) in the range of 400-4000 cm-1 using KBr pellets. Field emission scanning electron microscopes (FESEM) were performed by TESCAN MIRA (Czech Republic), to observe the surface morphologies of the samples. The electrical conductivities were measured using a standard four-probe set up connected to a keithly system comprising a voltmeter and a constant high current source (ASTM Standards, F43-93-Home made Iran).

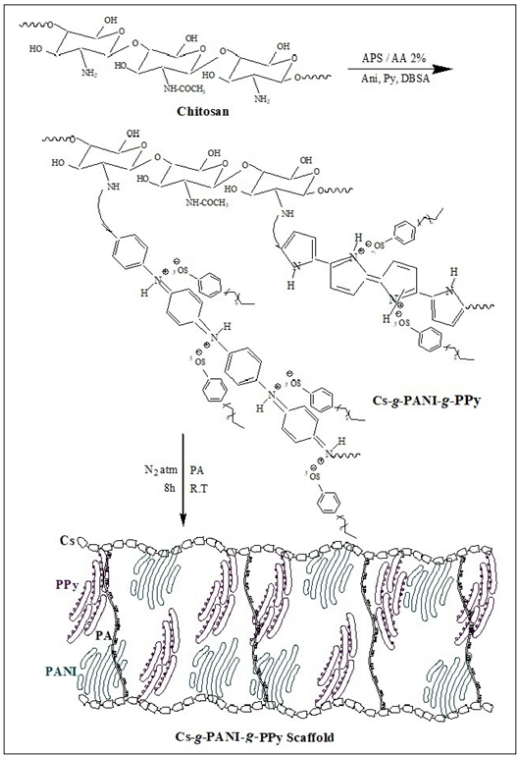

Figure 1: Schematic display of polymer scaffold preparation steps.

Antibacterial Testing Methodology: Detailed Protocols

For the disk diffusion assay (Kirby-Bauer), Mueller Hinton Agar (MHA) plates were swabbed uniformly with bacterial suspensions standardized to a 0.5 McFarland turbidity (≈1.5 × 10^8 CFU/mL). For the well-diffusion method, wells (5 mm diameter) were aseptically punched into the agar. Subsequently, 100 µL of a 500 µg/mL stock solution of the Cs-g-PANI-g-PPy nanofiber scaffold (disspersed/sonicated in sterile distilled water) was introduced into each well, delivering a final amount of 50 µg per well. For the direct surface application method, 50 µg of the solid scaffold material was carefully placed onto the surface of the pre-inoculated agar. Both setups, alongside positive (bacteria-only) and negative (sterility) controls, were incubated aerobically at 37°C for 18-24 hours. Zones of Inhibition (ZOI) were measured in millimeters from the edge of the well/scaffold material to the edge of the clear zone.

The Minimum Inhibitory Concentration (MIC) was determined via a broth microdilution assay in a 96-well plate. Two-fold serial dilutions of the scaffold extract were prepared in Mueller Hinton Broth (MHB) across the plate rows, yielding a concentration range of 5-80 µg/mL. Each well was then inoculated with 100

µL of the standardized bacterial suspension to achieve a final test concentration range. The plate was incubated at 37°C for 24 hours. The MIC was defined as the lowest concentration of the scaffold that resulted in no visible turbidity, indicating complete inhibition of bacterial growth. Optical Density (OD) at 600 nm was measured spectrophotometrically to calculate the precise Inhibition Activity (%).

Preparation of chitosan-nanofiber polyaniline and polypyrrole graft copolymer (Cs-g-PANI-PPy) scaffold

The grafting of PANI and PPy on chitosan was carried out in a 250 mL four-necked flask equipped with thermometer, condenser, stirrer and gas inlet by interfacial polymerization method. 0.5 g of Cs and 5.69 g (0.025 mol) APS in a 50 mL AA (2%) solution were dissolved and stirred well under nitrogen gas for one hour. Then 0.5 g DBSA was dissolved in 15 mL distilled water and was added to flask. In the other becher, 1 g (0.01 mol) aniline and 1 g (0.015 mol) pyyrole were dissolved in 30 ml chloroform and stirred with magnetic stirrer for 30 min and then was added above flask. The mixture was kept under N2 atmosphere and stir at 5°C for 2 hours. Then 0.5 g PA was added and was kept under N2 atmosphere and stir at room temperature for 8 hours. Finally, the black green solid disk was separated from interface of the immiscible solutions and washed several times by acetone and distilled water. Cs-g-PANI-g-PPy nanofiber scaffold was dried at 50-60°C for 24 hours.

Result and Discussion

Fourier-Transform Infrared (FTIR) Spectroscopy

Figure 2 shows the FTIR spectra of Cs-g-PANI-g-PPy nanofiber scaffold. The observed broad peak at 3544 cm^{-1} is corresponded to the symmetric stretching vibration of O-H groups of dopant, PA and Cs. The other observed broad and sharp peaks at 3413 and 3240 cm-1 are related to the symmetric stretching vibration modes of N-H groups of PANI and PPy. The shoulder peaks at 2926 and 2857 cm^{-1} are related with symmetric stretching modes of C-H aliphatic Cs and DBSA. The peaks at 1684 and 1627 cm^{-1} are assigned to sulfonic acid and P=O groups for DBSA and PA, respectivey. The specific peaks at 1559, 1490 and 1446 cm^{-1} are assigned to the characteristic C=C and C-N stretching of the quinoid and benzenoid rings of PANI and PPy.

The various “fingerprint” absorption patterns for P–O bending frequencies of the phytate was showed a broad peak at 1500–900 cm−1 range. Of course, this wavelength range is not very fixed and depends on the reaction environment and other compounds, which was seen here as a broad peak in the area of 1128 cm^{-1}. This peak has an overlap to peaks N-H and C-O stretching vibrations related to PANI, PPy and chitosan, too. The peaks at 838, 755 and 668 cm^{-1} are attributed to the p-disubstituted aromatic ring and aliphatic C-H out of plane bending. The peaks in 668 and 607 cm^{-1} ranges are the main characteristic of phytate, which is related two modes for the bending vibration of O-P-O. According to the mentioned data, it is inferred that the claimed polymer has been successfully synthesized.

Deeper FTIR Analysis

The FTIR spectrum provides compelling evidence for successful graft copolymerization and crosslinking. The broad peak at 3544 cm^{-1} signifies extensive hydrogen bonding involving the -OH groups of chitosan and phytic acid, a key interaction for hydrogel and scaffold formation. The distinct separation of N-H stretching vibrations into peaks at 3413 cm^{-1} and 3240 cm^{-1} is indicative of the presence of different amine environments—primarily the primary amines of chitosan and the secondary amines characteristic of the PANI and PPy backbone structures. The presence of sulfonic acid (S=O, 1684 cm^{-1}) and phosphoryl (P=O, 1627 cm^{-1}) peaks confirms the successful doping of the conducting polymers by DBSA and the ionic crosslinking of chitosan by phytic acid, respectively. The quintessential peaks of conducting polymers—the quinoid (C=N, ~1560 cm^{-1}) and benzenoid (C=C, ~1490 cm^{-1}) ring stretches—are clearly visible and slightly shifted compared to pure PANI or PPy homopolymers, suggesting π-π interactions and electronic coupling between the grafted chains and the chitosan backbone. The complex fingerprint region (1500-900 cm^{-1}) confirms the incorporation of the phytate anion, crucial for the scaffold's structural integrity.

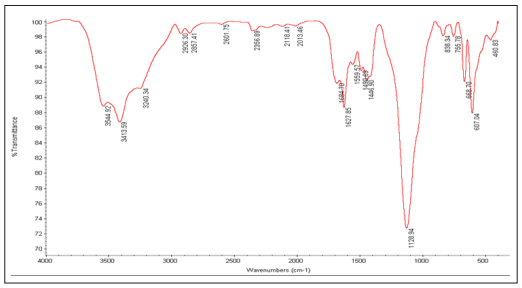

Figure 2: FTIR spectra of Cs-g-PANI-g-PPy nanofiber scaffold.

Field Emission Scanning Electron Microscopes (FESEM) Observation

The morphology, size of porous and distribution of Cs-g-PANI-g-PPy nanofiber as investigated by FESEM images. SEM images of Cs-g-PANI-g-PPy nanofiber scaffold with different sizes were displayed in Figure 3(a,b). The complete shape of the scaffold is shown in Figure 3a. In Figure 3a, the spongy form of the scaffold is quite clear. Average cluster and fibrous size of PANI was determined according to SEM analyses by using a microstructure measurement program and Minitab statistical software. As shown in Figure 3b, the size of the porous and holes of the scaffold is between 1-14 µm. According to Figures 3a, 3b and our past experiences [10], PANI is mostly seen as nanoclusters and PPy as nanofibers. The average size of these fibers is between 200-300 nm. The scaffold is almost uniform and completely spongy. Given this shape, bone repair applications can be predicted for it.

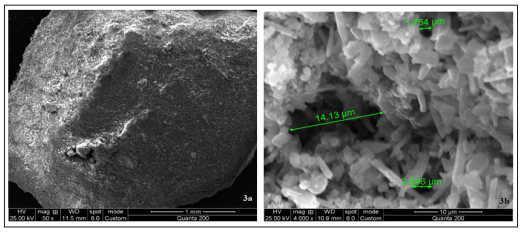

Figure 3: Field emission scanning electron microscopes (FESEM) images of Cs-g-PANI-g-PPy nanofiber scaffold a) the spongy form and b) the porous and holes form in different sizes

Morphological Advantages for Biomedical Application

The observed spongy, highly porous morphology with pore sizes ranging from 1-14 μm is not merely a structural outcome but a functionally critical feature. This architecture is ideal for biomedical applications for three primary reasons: (1) High Surface Area: The nanofibrous and porous structure offers an immense surface area, facilitating high loading capacity for therapeutic agents (e.g., antibiotics, growth factors) in drug delivery applications. (2) Cell Ingrowth and Vascularization: pore sizes in this range (typically 5-15 μm for cell migration and >100 μm for vascularization initiation) are known to promote the infiltration of cells like fibroblasts and osteoblasts, nutrient diffusion, and waste removal, which are essential for tissue regeneration and integration of the implant with the host tissue. (3) Exudate Absorption: In wound dressing applications, such a porous network can effectively absorb wound exudate while maintaining a moist healing environment.

Electrical Conductivity and Its Significance

The measured electrical conductivity of 0.151 S/cm for the Cs-g-PANI-g-PPy nanofiber scaffold is a significant value in the context of electro-active biomaterials. This conductivity is orders of magnitude higher than that of pure chitosan (an insulator) and substantially higher than many reported PANI or PPy-based biocomposites. This enhancement is attributed to a synergistic effect: the interfacial polymerization method promotes the growth of well-ordered, extended conjugated structures of both PANI and PPy on the chitosan template. Phytic acid acts as an efficient multi-site dopant, protonating the imine nitrogen atoms in the polymer chains and introducing charge carriers (polarons/bipolarons) that can delocalize along the combined π-conjugated system of the grafted copolymers. And of course, the role of the crosslinking agent also plays a role here, which is completely non-toxic compared to other crosslinking agents. This level of conductivity is critically important. It falls within a range that can significantly influence cellular behavior; applied electrical stimulation through such a scaffold can enhance neurite outgrowth in neural tissue engineering, accelerate fibroblast proliferation and collagen deposition in wound healing, and promote osteogenic differentiation in bone tissue engineering by mimicking the body's natural bioelectric signals.

Proposed Mechanism of Antibacterial Action

The potent antibacterial activity of the Cs-g-PANI-g-PPy scaffold is not attributable to a single mechanism but rather a combination of synergistic effects stemming from its unique composition:

- Membrane Disruption via Electrostatic Interaction: The protonated amine groups of chitosan and the positively charged nitrogen atoms in the doped PANI/PPy chains create a highly cationic surface. This facilitates strong electrostatic adhesion to the negatively charged phospholipids of bacterial cell membranes (e.g., lipoteichoic acids in gram-positive, lipopolysaccharides in gram-negative), leading to membrane destabilization, leakage of intracellular components, and eventual cell lysis [20].
- Reactive Oxygen Species (ROS) Generation: Conducting polymers like PANI and PPy can participate in redox reactions with molecular oxygen. The transfer of electrons from the bacterial respiratory chain or from the polymer itself to oxygen can generate cytotoxic reactive oxygen species (ROS), such as superoxide radicals ($O_2^{\bullet -}$) and hydrogen peroxide (H_2O_2). A surge in intracellular ROS levels causes oxidative stress, damaging proteins, lipids, and DNA, ultimately triggering bacterial cell death [21].
- Physical Interaction and Inhibition: The nanofibrous network can physically entrap bacteria, limiting their mobility and access to nutrients, thereby inhibiting colonial growth and biofilm formation. The leaching of bioactive components like oligomeric chitosan chains or doped monomer units may also contribute to the observed inhibition zones in the agar diffusion tests [22].

The generally higher efficacy against gram-negative bacteria, as observed, can be explained. While their outer membrane presents a barrier, its primary component, LPS, is highly anionic. The powerful electrostatic attraction to the cationic scaffold likely compromises the integrity of this outer membrane first, allowing the other mechanisms (ROS, physical disruption) to more effectively target the underlying thin peptidoglycan layer and cell membrane.

Efficiency and Grafting Percentage Determinations

Measuring the grafted percentage and product efficiency is very important in terms of polymer properties. Here, considering that we have two types of monomers, this value depends on various factors, such as the chemical potential of the monomers, concentration of monomers, type of initiator, dopant, reaction time and temperature. Their control can determine the final properties of the copolymer and cover wide aspects of different applications. Percentage of grafting in graft copolymer was measured by three methods: (a) the integration of the area under the peak; (b) by gravimetry and (c) by measurement of N% in copolymer [7,23].

$$W_1 = 0.50,\ W_2 = 0.87,\ W_3 = 0.88$$

$$\text{Grafting \%} = \frac{\text{weight of Cs-}g\text{-PANI-PPy-NF}}{\text{weight of chitosan}} \times 100$$

$$\text{Grafting \%} = \frac{W_3 - W_1}{W_1} \times 100$$

$$\text{Grafting \%} = \frac{0.88 - 0.50}{0.50} \times 100 = 76.00$$

$$\text{Efficiency \%} = \frac{\text{weight of Cs-}g\text{-PANI-PPy-NF}}{\text{weight of polymer grafted and homopolymers}} \times 100$$

$$\text{Efficiency \%} = \frac{W_3 - W_1}{W_2} \times 100$$

$$\text{Efficiency \%} = \frac{0.88 - 0.50}{0.87} \times 100 = 43.68$$

The weight of chitosan used is W1 (g) and the weight of graft copolymer and homopolymers are considered W2 (g). On the other hand, with continuous extraction with a suitable solvent, the homopolymer is separated from the reaction medium and the copolymer. Then the resulting final polymer was washed with ice methanol and dried slowly under vacuum and it was called W3 (g) (Cs-g-PANI-g-PPy-NF). The difference in (W3-W1) gives the weight of the grafted polymers (PANI and PPy). The difference in (W2-W3) gives the weight of the homopolymers PANI, PPy which gives W4 (g). Therefore, we can perform the following calculations to measure the grafting percentage and the efficiency percentage.

Determine the Antimicrobial Efficacy of Cs-g-PANI-g-PPy Nanofiber Scaffold

The disc diffusion agar dilution (Kirby-Bauer) for determination zone of inhibition (ZOI) and the micro dilution broth for determination of minimum inhibitory concentration (MIC) and percent of inhibition activity (IA%) were used to assay the antimicrobial activity of the Cs-g-PANI-g-PPy nanofiber scaffold against the bacterial suspensions as described by the Clinical and Laboratory Standards Institute (CLSI). These complementary methods provide quantitative (MIC/IA%) and spatial (ZOI) assessment of bactericidal efficacy, essential for evaluating novel polymeric antimicrobials.

The reference strains including Pseudomonas aeruginosa (ATCC 27853) and Klebsiella pneumonia ATCC 700603 as gram-negative and Staphylococcus aureus ATCC 29313 as gram-positive were examined to determine their susceptibility to polymer. The bacteria strains were inoculated in 10 mL of Luria-Bertani (LB) broth overnight at 37°C. Selection of representative gram-negative and gram-positive pathogens allows critical evaluation of the scaffold's spectrum against structurally distinct bacterial membranes, particularly the LPS barrier of gram-negative strains.

The strains were adjusted to 0.5 McFarland, with OD625 nm (0.08−0.13) which is equivalent to 108 CFU/mL. Bacterial suspensions were adjusted to a McFarland 0.5 turbidity standard corresponding to 1.5 × 108 colony forming unit per 1 mL (CFU/mL), which the OD625 nm should be to 0.08–0.13.

Inhibition zones of bacteria strains around the scaffold inoculation area by using the Kirby-Bauer test were considered antibiotic susceptibility. In the Kirby-Bauer test, Muller Hinton Agar (MHA) plates were inoculated with each bacterial suspension with a McFarland 0.5. A puncher created Wells (5 mm in diameter) in an MHA plate. Then, 100 µl of Cs-g-PANI-g-PPy nanofiber scaffold with a concentration 50 µg were loaded into each well in an MHA plate, and incubated overnight at 37◦C. It is noteworthy that in another method, 50 µg of scaffold components were inoculated on the surface of the MHA media without creating wells. Inhibition zones of bacteria strains around the scaffold inoculation area were considered antibiotic susceptibility. One plate was considered as a control without any inoculation of Cs-g-PANI-g-PPy nanofiber scaffold. ZOI is determined based on the presence or absence of a zone of inhibition surrounding the inoculation area. This direct surface application protocol specifically assesses the intrinsic diffusional properties and contact-mediated activity of the nanofibrous scaffold matrix.

The MIC was determined using the micro-broth dilution method by preparing a dilution series of the components in the 96-well microtiter plate. The diluted bacterial suspension (100 µL) was added to the 96-well plate containing the Cs-g-PANI-g-PPy nanofiber scaffold with different concentrations (5, 10, 20, 40, and 80 µg/mL) to each well to make a final volume of 200 µL. Plates were incubated at 35±2°C for 18–20 h in order to most scaffold/bacteria strain combinations. Mueller Hinton Broth (MHB) only or E. coli O157: H7 ATCC 43888 with MHB to the wells were used as negative and positive growth controls, respectively. At the end of the incubation, the optical density (OD) of wells was read at a wavelength of 600 nm by using a spectrophotometer. This quantitative method critically evaluates the scaffold's bacteriostatic/bactericidal thresholds across a physiologically relevant concentration gradient, essential for therapeutic dosing considerations. The inhibition activity (IA %) was calculated as follows: Inhibitory effect (%) = (OD control − OD sample)/OD control × 100.

OD sample and OD control are OD values of the bacterial strain alone and the bacterial strain and polymer mix, respectively. Notably, the potent IA% observed against K. pneumoniae and P. aeruginosa (exceeding 75% at 80 µg/mL) underscores the scaffold's ability to overcome intrinsic resistance mechanisms in gram-negative bacteria. Figure 4 represents the antimicrobial activity of scaffold (50 µg) against standard bacteria strains.

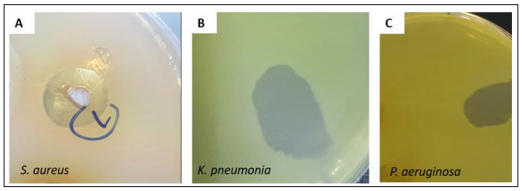

Figure 4: Antimicrobial activity of the tested Cs-g-PANI-PPy nanofiber scaffold against bacteria strains. (50 µg of polymer was loaded into each well or on the surface of an MHA plate)

The mean diameters of ZOI against P. aeruginosa, K. pneumoniae, and S. aureus were 12.5, 11.6 and 9.4 mm, respectively. The different concentrations of the scaffold have inhibited the growth of bacteria strains, significantly. However, Cs-g-PANI-g-PPy nanofiber scaffold was able to inhibit the growth of bacteria in concentrations of above 10 µg. Table 1 and Figure 5 illustrates the inhibition activity of the tested Cs-g-PANI-g-PPy nanofiber scaffold against the bacteria strains. The dose-dependent IA% values (Table 1) reveal a distinct structure-activity relationship, where the multi-grafted copolymer architecture significantly enhances efficacy against gram-negative pathogens – an effect attributed to synergistic disruption of their lipopolysaccharide-rich outer membranes.

The polymer composites exhibit the highest microbial inhibition activity against negative gram bacteria. Inhibitory effect of polymer composite in its higher concentration against k. pneumonia was 0.88% followed by P. aeruginosa (0.76%) and S. aureus (0.48%). This polymer in concentrations of 60 to 80 µg had an almost similar antimicrobial effect. Figure 6 shows the

mechanisms of bacterial death by Cs-g-PANI-g-PPy nanofiber scaffold. These spatial inhibition patterns correlate directly with the MIC/IA% data, confirming dual antimicrobial mechanisms: contact-mediated membrane disruption (evident in ZOI) and soluble bioactive component diffusion (reflected in broth assays).

Table 1: Inhibition activity of Cs-g-PANI-g-PPy nanofiber scaffold against bacterial strains

Concentration of scaffold (µg)	Inhibition activity (I %)		
	K. pneumonia ATCC 700603	P. aeruginosa ATCC 27853	S. aureus ATCC 29313
Control*	0.01	0.03	0.01
0	0.01	0.01	0.02
5	0.13	0.10	0.06
10	0.35	0.29	0.23
20	0.57	0.53	0.29
40	0.78	0.71	0.39
80	0.88	0.76	0.48
*OD control is the OD value of the bacterial strain without polymer			

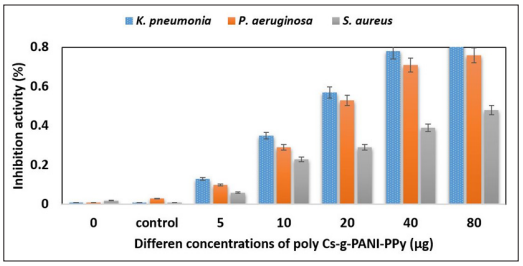

Figure 5: Inhibition activity of Cs-g-PANI-g-PPy nanofiber scaffold against bacterial strains

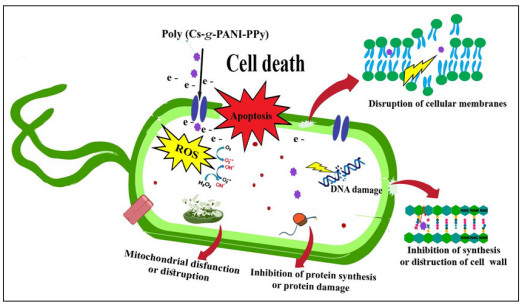

Figure 6: Mechanisms of bacterial death by Cs-g-PANI-g-PPy nanofiber scaffold (ROS; Reactive oxygen species)

Conclusion

In past research, we have shown that conducting polymers play a good role as antibacterial. In the current research, we prepared a new conducting polymer scaffold obtained from the multi-grafted copolymer of chitosan with PANI and PPy, which, in addition to the ability to carry drugs, has a very good ability to kill various bacteria. This multi-grafted architecture significantly enhances bactericidal efficacy against resistant strains by synergistically disrupting bacterial membranes through electrostatic interactions and redox cycling. In addition, harmful effects caused by elevated oxygen reactive species (ROS) induce cell death. The presence of the additional protection layer of the outer membrane (lipopolysaccharide; LPS) in gram-negative bacteria can likely raise the inhibitory effect of the polymer. As well as this polymer composition with positive charges binds to the negatively charged LPS to interfere with bacterial activities. Antibacterial activity of Cs-g-PANI-g-PPy nanofiber scaffold against selected bacteria may be due to the reduced concentration of low molecular weight byproducts. On the other hand, the movement of electrons and the movement of counter ions (dopants-like surfactants) on the surface of the polymer help to prevent the growth of bacteria and destroy the cell wall. The growth of P.aeruginosa, K. pneumoniae, and S. aureus exposed to scaffold was inhibited. Probably, this combination has the capacity to eradicate methicillin-resistant S. aureus (MRSA) and other multidrug-resistant (MDR) bacteria. The inherent conductivity of this nanofibrous scaffold further potentiates its therapeutic utility, enabling electrical stimulation-enhanced tissue regeneration and localized electrochemotherapy modalities. This experience showed that the prepared scaffold has a good ability to restore skin and bones and help in the treatment of various cancers, including skin and breast cancer. Future work will focus on in-vivo biocompatibility studies, loading and release kinetics of model drugs (e.g., antibiotics, anticancer agents), and evaluating the scaffold's performance under externally applied electrical stimulation to fully harness its potential as a next-generation active implantable device. This multi-grafted architecture significantly enhances bactericidal efficacy against resistant strains by synergistically disrupting bacterial membranes through electrostatic interactions and redox cycling.

Author Contributions

Conceptualization: Sama sadat Hosseini, Seyed Hossein Hosseini
Investigation: Sama sadat Hosseini, Seyed Hossein Hosseini, Seyed Amirreza Dehghani, Hamid Arabloo
Methodology: Sama sadat Hosseini, Seyed Hossein Hosseini,
Formal analysis: Seyed Hossein Hosseini,
Writing – original draft: Seyed Hossein Hosseini,
Writing – review & editing: Sama sadat Hosseini, Seyed Amirreza Dehghani, Hamid Arabloo
All authors have read and agreed to the published version of the manuscript.

Acknowledgments: Not applicable

Funding: We acknowledge financial support from the Nika Pooyesh Industrial Research Institute.

Data Availability Statement: Data underlying the results presented in this paper are not publicly available at this time but may be obtained from the authors upon reasonable request.

Ethics approval and consent to participate: Not applicable

Consent for publication: Not applicable

Conflicts of Interest: The authors declare no conflicts of interest.

References

1. Hosseini SH, Hosseini SS, Hatami R. Chemical and Electrochemical Graft Copolymerization of Nano Porose Polyaniline onto Polyphosphazene and Application It as Sensor for Some of Insecticides. International Journal of Nanomaterials & Molecular Nanotechnology. 2023. 5:146.
2. Raj GK, Singh E, Hani U, Ramesh K, Talath S, et al. Conductive polymers and composites-based systems: An incipient stride in drug delivery and therapeutics realm. Journal of Controlled Release. 2023. 355: 709 -729.
3. Ajmal Z, Naciri Y, Ahmad M. Hsini A, Bouziani A, et al. Use of conductive polymer-supported oxide-based photocatalysts for efficient VOCs & SVOCs removal in gas/liquid phase. Journal of Environmental Chemical Engineering. 2023. 11: 108935.
4. Guchait S, Zhong Y, Brinkmann M. High-Temperature Rubbing: An Effective Method to Fabricate Large-Scale Aligned Semiconducting and Conducting Polymer Films for Applications in Organic Electronics. Macromolecules. 2023. 56: 6733-6757.
5. Yu H, Wang Y, Zou X, Yin J, Shi X, et al. Improved photovoltaic performance and robustness of all-polymer solar cells enabled by a polyfullerene guest acceptor. Nature Communications. 2023. 14: 2323.
6. Beyazay E, Karabul Y, Korkut SE, Kılıç M, Özdemir ZG. Multifunctional PCz/BaO nanocomposites: Ionizing radiation shielding ability and enhanced electric conductivity. Progress in Nuclear Energy. 2023. 155: 104521.
7. Hosseini SS, Hosseini SH, Hajizade A. Preparation of graft copolymer of chitosan-poly ortho-toluidine for antibacterial properties Heliyon. 2024. 10: e33960.
8. Dudun AA, Chesnokova DV, Voinova VV, Bonartsev AP, Bonartseva GA. Changes in the Gut Microbiota Composition during Implantation of Composite Scaffolds Based on Poly (3-hydroxybutyrate) and Alginate on the Large-Intestine Wall. Polymers. 2023. 15: 3649.
9. Haki M, Shamloo A, Eslami SS, Sadeghi MMF, Maleki S, et al. Fabrication and characterization of an antibacterial chitosan-coated allantoin-loaded NaCMC/SA skin scaffold for wound healing applications. International Journal of Biological Macromolecules. 2023. 253: 127051.
10. Zhang T, Qin X, Gao Y, Kong D, Jiang Y, et al. Functional chitosan gel coating enhances antimicrobial properties and osteogenesis of titanium alloy under persistent chronic inflammation. Frontiers in Bioengineering and Biotechnology. 2023. 11: 1118487.
11. Desai N, Rana D, Salave S, Gupta R, Patel P, et al. Chitosan: A Potential Biopolymer in Drug Delivery and Biomedical Applications. Pharmaceutics. 2023;15: 1313.
12. Azaman FA, Zhou K, Blanes-Martínez MM, Fournet BM, Devine DM. Bioresorbable Chitosan-Based Bone Regeneration Scaffold Using Various Bioceramics and the Alteration of Photoinitiator Concentration in an Extended UV Photocrosslinking Reaction. Gels. 2022. 8: 696.
13. Hosseinkhani H. Biomedical Engineering: Materials, Technology, and Applications 1st Edition, Weinheim, Germany: Wiley-VCH. 2022.
14. Hosseini SH, Dolabi MB. Preparation of Multi-absorbers Nanocomposite of Regions X–Ku Band and Thermal Infrared Based on BaTiO3-WO3, Ba-Sr-Mn-La Ferrite and Polyaniline. Journal of Electronic Materials. 2022. 51: 4079-4094.
15. Gupta S, Tripathi A. Chitosan-Polyaniline hybrids: Recent advances in electrochemical sensors, antimicrobial activity, and biomedical applications, International Journal of Biological Macromolecules. 2024. 254: 127853.
16. Wang L, Li Y. Electroactive Nanofibrous Scaffolds Based on Chitosan and Conductive Polymers for Enhanced Neuronal Differentiation under Electrical Stimulation, ACS Applied Materials & Interfaces. 2024. 16: 5555-5568.
17. Karim MR, Islam S. Phytic Acid: A Multi-Functional Bio-Based Crosslinker and Dopant for Sustainable Conductive Polymer Composites, Carbohydrate Polymers. 2024. 324: 121487.
18. Kiamarzi M, Attar MM, Hosseini SH. Preparation of X-ray shielding nanocomposites based on cadmium selenide-zinc oxide and polyaniline with core-shell structure, Surfaces and Interfaces. 2025. 56: 105545.
19. Hosseini SH, Falsafi A. Preparation of soft-hard X-ray absorption nanocomposites using PbS, PbSe coated on SWCNTs based polyaniline, International Journal of Physical Sciences. 2025. 20: 12-25.
20. Zhang Y, Li X, Wang Z, et al. Cationic Chitosan-Modified Nanoparticles Effectively Target and Disrupt Bacterial Membranes through Electrostatic Interactions. ACS Applied Materials & Interfaces. 2024. 16: 5760-5771.
21. Chen L, Kumar A. Polyaniline-Based Nanocomposites as Potent ROS Generators for Advanced Antibacterial Therapies. Advanced Healthcare Materials. 2024. 13: 2303250.
22. Wang Y, Fernandez R, Li B. Engineered Nanofibrous Scaffold with Dual-Functionality for Physical Capturing and Photothermal Killing of Bacteria to Prevent Biofilm Formation. Biomaterials Science. 2024. 12: 2258-2272.
23. Hosseini SH. Ammonium Persulphate Initiated Graft Copolymerization of Aniline onto Chitosan-A Comparative Kinetic Study. Int. J. Adv. Sci. Eng. 2021. 7: 1975-1982.